23rd INTERNATIONAL CONFERENCE ON GENERAL RELATIVITY AND GRAVITATION
July 3-8, 2022 Beijing, China

Circular Geodesics Around A Rotating Black Hole

Dr. Sehrish Iftikhar, Assistant Professor Mathematics, LCWU, Pakistan.

Abstract: This poster is devoted to study the circular motion of neutral test particles orbiting near Kerr–Newman black hole in the presence of quintessential dark energy and cosmological constant We limit our analysis to the equatorial plane and explore the properties of both time-like and null geodesics. We also discuss the stable regions with respect to the horizons, radius of photon sphere and the so called static radius. We have shown that the stable points are always less than the static radius while they exceed the radius of photon orbit. The energy extraction, negative energy state and energy gain during the Penrose process is also discussed. It is found that more energy can be gained during the Penrose process in the presence of dark energy as compared to the charge and spin of the said black hole. This research work has been published in [Iftikhar, S. and Shehzadi, M.: Eur. Phys. J. C **79**(2019) 473].

Equations of Motion

The Kerr Newman de Sitter black hole in quintessential dark energy (KNdSQ BH) is the solution of Einstein-Maxwell equations and the line element corresponding to this BH is given as [Xu, Z. and Wang, J.: Phys. Rev. D **95**(2017)064015]

$$
\begin{aligned}
ds^2 &= \frac{\rho^2}{\Delta_r}dr^2 + \frac{\rho^2}{\Delta_\theta}d\theta^2 + \frac{\Delta_\theta \sin^2\theta}{\rho^2}(a\frac{dt}{\Sigma} \\
&- (r^2+a^2)\frac{d\phi}{\Sigma})^2 - \frac{\Delta_r}{\rho^2}(\frac{dt}{\Sigma} - a\sin^2\theta\frac{d\phi}{\Sigma})^2,
\end{aligned}
$$

where

$$\Delta_r = r^2 + a^2 + Q^2 - 2Mr - \alpha r^{1-3\omega} - \frac{\Lambda}{3}(r^2+a^2)r^2,$$

$$\Delta_\theta = 1 + \frac{a^2}{3}\Lambda\cos^2\theta, \quad \Sigma = 1 + \frac{a^2}{3}\Lambda, \quad \rho^2 = r^2 + a^2\cos^2\theta.$$

The motion of a test particle in the equatorial plane can be described by the following Lagrangian

$$
\begin{aligned}
2\mathcal{L} &= -\left(\frac{\Delta_r - a^2}{r^2\Sigma^2}\right)\dot{t}^2 - 2a\left(\frac{r^2+a^2-\Delta_r}{r^2\Sigma^2}\right)\dot{t}\dot{\phi} + \frac{r^2}{\Delta_r}\dot{r}^2 + \frac{r^2}{\Delta_\theta}\dot{\theta}^2 \\
&+ \left(\frac{(r^2+a^2)^2 - a^2\Delta_r}{r^2\Sigma^2}\right)\dot{\phi}^2. \qquad (1)
\end{aligned}
$$

The generalized momenta are calculated as

$$
\begin{aligned}
-p_t &= -\left(\frac{\Delta_r - a^2}{r^2\Sigma^2}\right)\dot{t} - a\left(\frac{r^2+a^2-\Delta_r}{r^2\Sigma^2}\right)\dot{\phi} = E, \qquad (2)\\
p_\phi &= \left(\frac{(r^2+a^2)^2 - a^2\Delta_r}{r^2\Sigma^2}\right)\dot{\phi} - a\left(\frac{r^2+a^2-\Delta_r}{r^2\Sigma^2}\right)\dot{t} = L, \qquad (3)\\
p_r &= \frac{r^2}{\Delta_r}\dot{r}. \qquad (4)
\end{aligned}
$$

The Hamiltonian can be written as

$$H = p_t\dot{t} + p_\phi\dot{\phi} + p_r\dot{r} - \mathcal{L}.$$

For KNdSQ BH, it takes the following form

$$
\begin{aligned}
2H &= -\left[\left(\frac{\Delta_r - a^2}{r^2\Sigma^2}\right)\dot{t} - a\left(\frac{r^2+a^2-\Delta_r}{r^2\Sigma^2}\right)\dot{\phi}\right]\dot{t} + \frac{r^2}{\Delta_r}\dot{r}^2 \\
&+ \left[\left(\frac{(r^2+a^2)^2 - a^2\Delta_r}{r^2\Sigma^2}\right)\dot{\phi} - a\left(\frac{r^2+a^2-\Delta_r}{r^2\Sigma^2}\right)\dot{t}\right]\dot{\phi} \\
&= -E\dot{t} + L\dot{\phi} + \frac{r^2}{\Delta_r}\dot{r}^2 = \epsilon = \text{constant},
\end{aligned}
$$

Solving Eq.(2) and (3), we have

$$
\begin{aligned}
\dot{t} &= \frac{\Sigma^2}{r^2\Delta_r}\left[aL\left(r^2+a^2-\Delta_r\right) - E\left((r^2+a^2)^2 - a^2\Delta_r\right)\right], \qquad (6)\\
\dot{\phi} &= \frac{\Sigma^2}{r^2\Delta_r}\left[a\left(E(r^2+a^2) - aL\right) - \Delta_r\left(aE - L\right)\right]. \qquad (7)
\end{aligned}
$$

Substituting Eqs.(6) and (7) into (5), we obtain the radial equation of motion

$$
\begin{aligned}
\dot{r}^2 &= E^2 + \frac{2M}{r^3}(L-aE)^2 + \frac{\Lambda}{3}(L-aE)^2 - \frac{Q^2}{r^4}(L-aE)^2 \\
&+ \alpha(L-aE)^2 r^{-3(1+\omega)} - \frac{1}{r^2}(L-aE) \\
&\times \left[aE + L - \frac{\Lambda}{3}(L-aE)a^2\right] - \frac{\Delta_r}{r^2}\epsilon. \qquad (8)
\end{aligned}
$$

Null Geodesics

Here, we discuss the case of null geodesics, i.e., $\epsilon = 0$ in Eq.(8) , introducing impact parameter $D = \frac{L_c}{E_c}$ *and considering the general case* $L \neq aE$. *For* $\omega = -\frac{2}{3}$, *we get*

$$
\begin{aligned}
&r_c^2(6Q^2 + r_c(-9M + r_c(3 + a^2\Lambda))) \\
&\pm 2\sqrt{3}a\sqrt{r_c^4[3Mr_c - 3Q^2 - r_c^3(3\alpha + \Lambda)]} = 0,
\end{aligned}
$$

For $\omega = -\frac{1}{2}$, *we get*

$$
\begin{aligned}
&r_c\left(r_c\left(4\left(a^2\Lambda + 3\right) - 6r_c(2\alpha + \Lambda) + 3\alpha\sqrt{r_c}\right) - 36M\right) + 24Q^2 \\
&\pm 4a\sqrt{36Mr_c - 36Q^2 - 9\alpha r_c^{5/2} + 6\Lambda r_c^3} = 0.
\end{aligned}
$$

Table 1: Photon orbits r_{po1} (direct rotating) for $\omega = -\frac{2}{3}$.

a	r_{po1}	Q	r_{po1}	α	r_{po1}
0	2.82288	0	2.49424	0	2.28096
0.1	2.69902	0.3	2.42205	0.0005	2.28187
0.2	2.56866	0.4	2.36288	0.05	2.38568
0.3	2.43032	0.5	2.32288	0.16	2.89882

Table 2: Photon orbits r_{po2} (counter rotating) for $\omega = -\frac{2}{3}$.

a	r_{po2}	Q	r_{po2}	α	r_{po2}
0	2.82288	0	3.43065	0	3.27222
0.1	2.94129	0.3	3.37503	0.0005	3.13627
0.2	3.05507	0.4	3.33038	0.05	3.43065
0.3	3.16481	0.5	3.271	0.16	2.89882

Table 3: Photon orbits r_{po1} (direct rotating) for $\omega = -\frac{1}{2}$.

a	r_{po1}	Q	r_{po1}	α	r_{po1}
0	2.8265	0	2.49642	0	2.28096
0.1	2.70219	0.3	2.42415	0.0005	2.2838
0.2	2.5714	0.4	2.36483	0.05	2.65816
0.3	2.43266	0.5	2.28381	0.16	2.48792

Table 4: Photon orbits r_{po2} (counter rotating) for $\omega = -\frac{1}{2}$.

a	r_{po2}	Q	r_{po2}	α	r_{po2}
0	2.8265	0	3.43649	0	3.27222
0.1	2.94539	0.3	3.38079	0.0005	3.27662
0.2	3.05965	0.4	3.33608	0.05	3.91084
0.3	3.1699	0.5	3.27662	0.16	3.93655

Time-like Geodesics

For time-like geodesics, we take $\epsilon = -1$. Consequently, radial equation takes the form

$$
\begin{aligned}
\dot{r}^2 &= E^2 + \frac{2M}{r^3}(L-aE)^2 + \frac{\Lambda}{3}(L-aE)^2 - \frac{Q^2}{r^4}(L-aE)^2 \\
&+ \alpha(L-aE)^2 r^{-3(1+\omega)} \\
&- \frac{1}{r^2}(L-aE)\left[aE + L - \frac{\Lambda}{3}(L-aE)a^2\right] - \frac{\Delta_r}{r^2}. \qquad (15)
\end{aligned}
$$

In the general ($L \neq aE$), following [Chandrasekhar, S.: The Mathematical Theory of Black Holes (Oxford University Press, 1983)], we substitute $x = L - aE$ in the radial equation (Eq.(15))

$$F(r) = r^4\dot{r}^2 = x^2(a^2 - \Delta_r) - 2aEr^2x + r^4E^2 - r^2\Delta_r. \qquad (17)$$

Differentiating with respect to *r*, the above equation takes the form

$$F'(r) = -4aErx + 4r^3E^2 - r^2\Delta'_r - 2r\Delta_r - x^2\Delta'_r. \qquad (18)$$

Combining Eqs.(17)-(18) and taking *F(r) = 0 = F'(r)*, we obtain energy and angular momentum, such as

$$E = \frac{1}{r\sqrt{\chi_\mp}}\left(\Delta_r - a^2 \mp \sqrt{a^4 - a^2\Delta_r + \frac{a^2r}{2}\Delta'_r}\right).$$

$$L = x + aE = \frac{1}{r\sqrt{\chi_\mp}}\left[\left(\Delta_r - a^2 - r^2\right)a \mp \left(r^2 + a^2\right)\sqrt{a^2 + \frac{r}{2}\Delta'_r - \Delta_r}\right]$$

where

$$\chi_\mp = 2\left(\Delta_r - a^2 - \frac{r}{4}\Delta'_r\right) \mp a\sqrt{4\left(a^2 - \Delta_r\right) + 2r\Delta'_r}.$$

The angular velocity for test particles turns out to be

$$\Omega = \frac{\dot{\phi}}{\dot{t}} = \frac{\mp\sqrt{a^2 + \frac{r}{2}\Delta'_r - \Delta_r}}{r^2 \mp \sqrt{a^4 - a^2\Delta_r + \frac{r}{2}a^2\Delta'_r}}.$$

By taking into account the expressions of energy as well as angular momentum, we found two reality conditions for the existence of the circular orbits. The first one is given as the following relation

$$y \leq y_s \equiv \frac{1}{2}r^{-4-3w}(\alpha r - 2Q^2r^{3w} + 2r^{1+3w} + 3\alpha r),$$

here, y=$\frac{\Lambda M^2}{3}$ and $M = 1$ (for the sake of simplicity). The above equation establish the notion of "static radius" which can be obtained from

$$-4Q^2 + 2r(2 + \alpha r^{-3w}(1 + 3w)) = 4r^4y$$

The second restriction on the existence of circular orbits is given as

$$2\left(\Delta_r - a^2 - \frac{r}{4}\Delta'_r\right) \mp a\sqrt{4\left(a^2 - \Delta_r\right) + 2r\Delta'_r} \geq 0.$$

23rd INTERNATIONAL CONFERENCE ON GENERAL RELATIVITY AND GRAVITATION
July 3-8, 2022 Beijing, China

Circular Geodesics Around A Rotating Black Hole

Dr. Sehrish Iftikhar, Assistant Professor Mathematics,
Lahore College for Women University, Pakistan.

Analysis of The Effective Potential

The radial equation of motion can be written as [Misner, C.W., Thorne, K.S. and Wheeler, J.A. Gravitation (W.H. Free- man, New York, 1973)]

$$\left(\frac{dr}{d\tau}\right)^2 + U_{eff} = E^2$$

where,

$$\begin{aligned} U_{eff} \;=\; & \frac{1}{r^2}(L-aE)\left[aE+L-\frac{\Lambda}{3}(L-aE)\,a^2\right]-\frac{2M}{r^3}(L-aE)^2 \\ - \; & \frac{\Lambda}{3}(L-aE)^2+\frac{Q^2}{r^4}(L-aE)^2-\alpha(L-aE)^2 r^{-3(1+\omega)}+\frac{\Delta_r}{r^2}\epsilon. \end{aligned}$$

The effective potential must attain minimum values for the case of stable circular orbits

$$\frac{\partial^2 U_{eff}}{\partial^2 r}\Big|_{r=r_0} > 0.$$

Plots of The Effective Potential

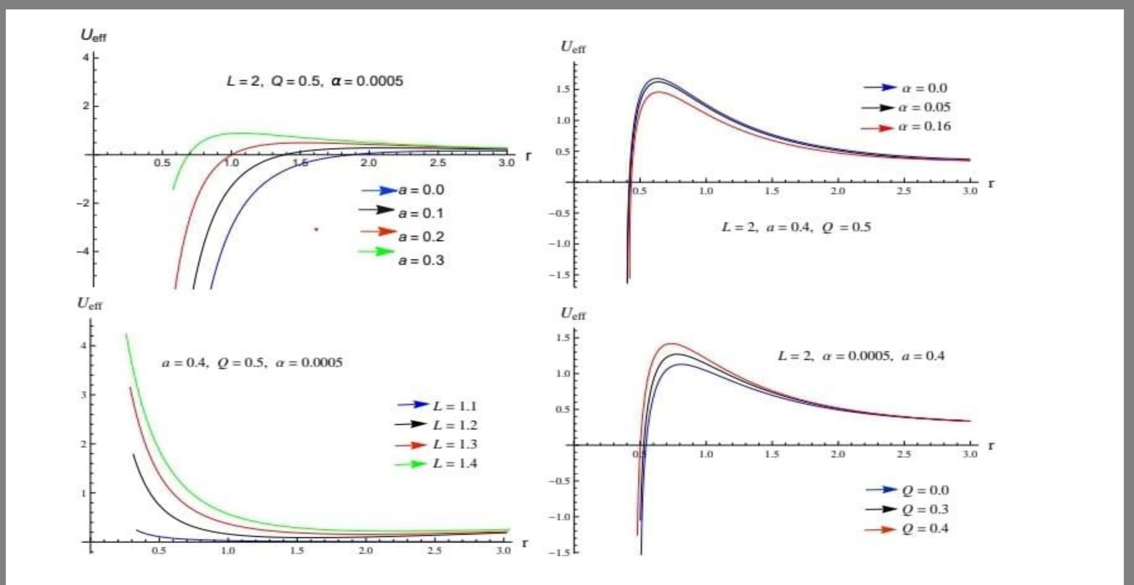

Figure 1 Plots of effective potential for null geodesics as a of function of r for $\omega=-\frac{2}{3}$.

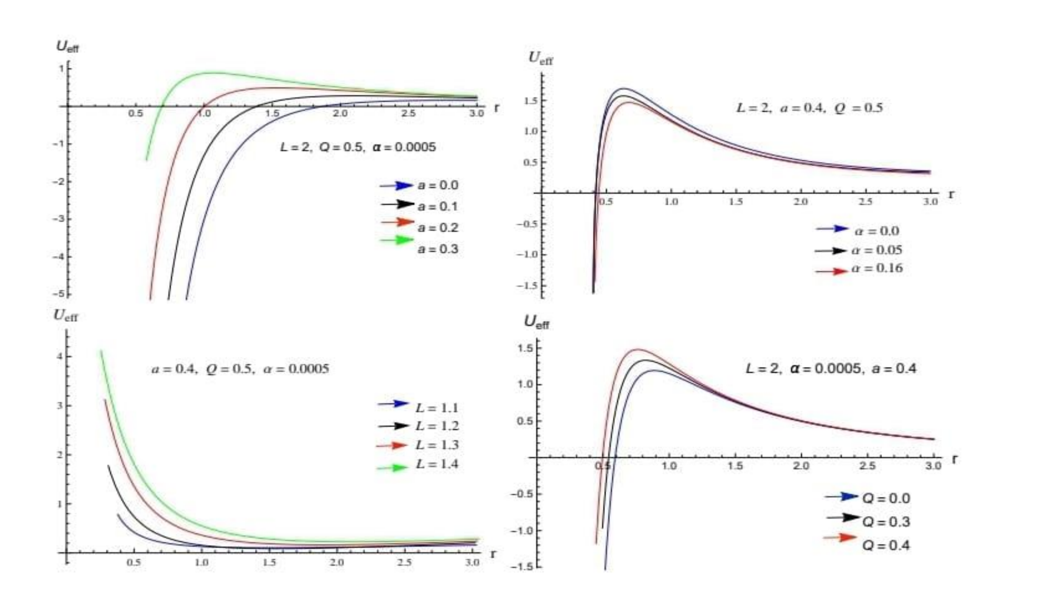

Figure 2 Plots of effective potential for null geodesics as a function of r for $\omega=-\frac{1}{2}$.

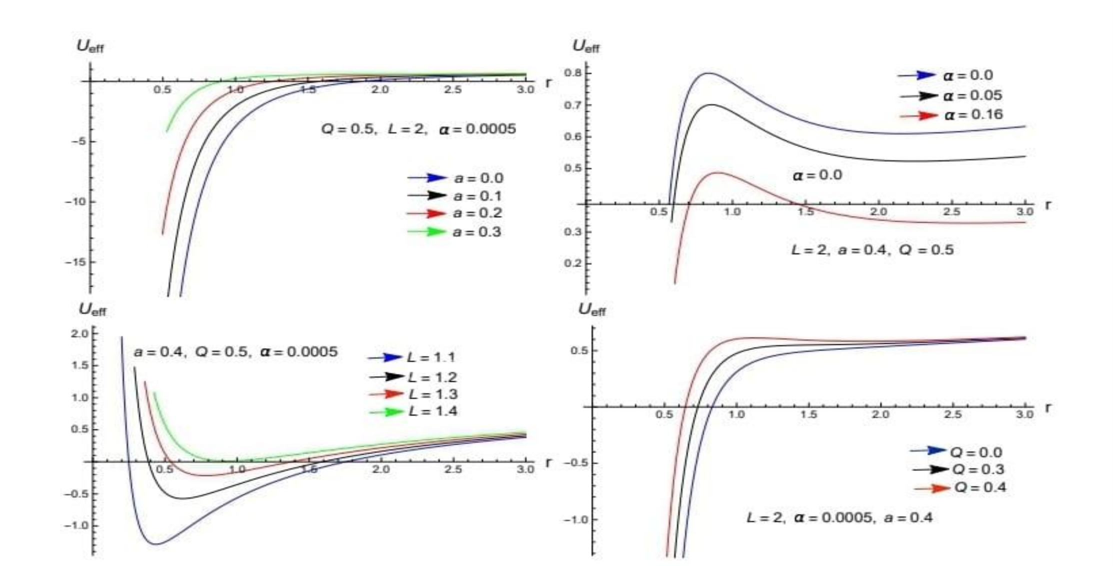

Figure 3 Plots of effective potential for time-like geodesics as a of function of r for $\omega=-\frac{2}{3}$.

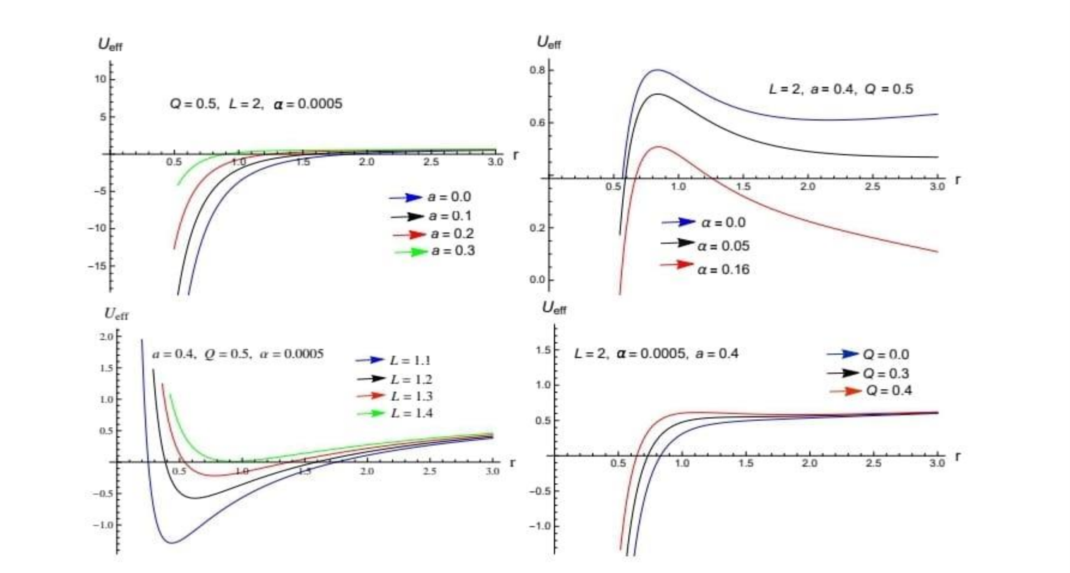

Figure 4 Plots of effective potential for time-like geodesics as a function of r for $\omega=-\frac{1}{2}$.

Analysis of the Radii

Table 5: Static radius for $\omega=\frac{-2}{3}$.

Q	r_s	α	r_s
0	53.4522	0	53.4072
0.3	19.9548	0.0005	19.8738
0.4	18.1769	0.05	6.19564
0.5	18.1311	0.16	4.4032

Table 6: Static radius for $\omega=\frac{-1}{2}$.

Q	r_s	α	r_s
0	39.9991	0	46.3992
0.3	35.416	0.0005	39.9833
0.4	35.4113	0.05	18.3978
0.5	35.4053	0.16	8.37896

Table 7: Inner (r_{h-}) and outer (r_{h+}) for $\omega=\frac{-2}{3}$.

a	r_{h-}	r_{h+}	Q	r_{h-}	r_{h+}	α	r_{h-}	r_{h+}
0	0.133973	1.8674	0	0.0834843	1.9179	0	0.231885	1.76811
0.1	0.139765	1.86161	0.3	0.133973	1.8674	0.0005	0.231877	1.76947
0.2	0.157382	1.84398	0.4	0.175375	1.82599	0.05	0.231051	1.91934
0.3	0.187591	1.81377	0.5	0.231877	1.76947	0.16	0.229269	2.44322

Table 8: Inner (r_{h-}) and outer (r_{h+}) horizons for $\omega=\frac{-1}{2}$.

a	r_{h-}	r_{h+}	Q	r_{h-}	r_{h+}	α	r_{h-}	r_{h+}
0	0.133974	1.8679	0	0.0834847	1.91844	0	0.231885	1.76811
0.1	0.139767	1.86211	0.3	0.133974	1.8679	0.0005	0.187591	1.81377
0.2	0.157384	1.84447	0.4	0.175377	1.82647	0.05	0.231482	1.992830
0.3	0.187594	1.81424	0.5	0.231881	1.76992	0.16	0.230609	2.45459

Table 9: Cosmological horizon r_c for $\omega=\frac{-2}{3}$.

a	r_c	Q	r_c	α	r_c
0	4×10^6	0	4×10^6	0	1.51911×10^8
0.1	4×10^6	0.3	4×10^6	0.0005	4×10^6
0.2	4×10^6	0.4	4×10^6	0.05	395.972
0.3	4×10^6	0.5	4×10^6	0.16	34.7164

Table 10: Cosmological horizon r_c for $\omega=\frac{-1}{2}$.

a	r_c	Q	r_c	α	r_c
0	19.98×10^2	0	19.98×10^2	0	1.51911×10^8
0.1	19.98×10^2	0.3	19.98×10^2	0.0005	4×10^6
0.2	19.98×10^2	0.4	19.98×10^2	0.05	17.7757
0.3	19.98×10^2	0.5	19.98×10^2	0.16	3.69231×10^5

Study of Stable Regions

In view of figures 1-2 and using tables 1-10

- For the variation of α, the stable points $(r\approx 1.63, 1.7, 1.8)$ lie in the region $r_{h-}<r_{h+}<r<r_s<r_c$, when $\omega=\frac{-2}{3}$, $\frac{-1}{2}$
- For the variation of Q, the stable points $(r\approx 1.5, 1.6, 1.62)$ lie in the region $r_{h-}<r_{h+}<r<r_s<r_c$ when $\omega=\frac{-2}{3}$, $\frac{-1}{2}$
- For the variation of L, the stable points $(r\approx 0.42, 0.6, 0.75, 0.8)$ lie in the region $r_{h-}<r_{h+}<r<r_s<r_c$ when $\omega=\frac{-2}{3}$, $\frac{-1}{2}$

- For the variation of Q, the stable points $(r\approx 2.67)$ lie in the region $r_{h-}<r_{h+}<r_{po_1}<r<r_{po_2}<r_s<r_c$, when $\omega=\frac{-2}{3}$, $Q=0,0.3,0.4$ whereas $r_{h-}<r_{h+}<r<r_{po_1}<r_{po_2}<r_s<r_c$, when $\omega=\frac{-2}{3}$, $Q=0.5$ and $r_{h-}<r_{h+}<r_{po_1}<r<r_{po_2}<r_s<r_c$, when $\omega=\frac{-1}{2}$
- For the variation of $L=1.1$ and $L=1.2, 1.3, 1.4$, the stable points $r\approx 0.7$ and $r\approx 1.65$ lie in the region $r_{h-}<r_{h+}<r<r_{po_1}<r_{po_2}<r_s<r_c$, when $\omega=\frac{-2}{3}$ and $\omega=\frac{-1}{2}$

In view of figures 3-4 and using tables 5-10

- For the variation of a, the stable points $(r\approx 1.99)$ lie in the region $r_{h-}<r_{h+}<r<r_{po_1}<r_{po_2}<r_s<r_c$
- For the variation of α, the stable points $(r\approx 2.6)$ lie in the region $r_{h-}<r_{h+}<r_{po_1}<r<r_{po_2}<r_s<r_c$, when $\omega=\frac{-2}{3}$, $\alpha=0, 0.0005, 0.05$ and $r_{h-}<r_{h+}<r<r_{po_1}<r_{po_2}<r_s<r_c$, when $\omega=\frac{-2}{3}$, $\alpha=0.16$ as well as $r_{h-}<r_{h+}<r<r_{po_1}<r_{po_2}<r_s<r_c$, when $\omega=\frac{-1}{2}$, $\alpha=0, 0.0005, 0.05$ and $r_{h-}<r_{h+}<r_{po_1}<r<r_{po_2}<r_s<r_c$, when $\omega=\frac{-1}{2}$, $\alpha=0.16$

Circular Geodesics Around A Rotating Black Hole

Dr. Sehrish Iftikhar, Assistant Professor Mathematics,
Lahore College for Women University, Pakistan.

23rd INTERNATIONAL CONFERENCE ON GENERAL RELATIVITY AND GRAVITATION
July 3-8, 2022 Beijing, China

The Penrose Process

Following [Chandrasekhar, S.: The Mathematical Theory of Black Holes (Oxford University Press, 1983)], we study the Penrose process for KNdQ BH. Using the radial equation, we get

$$E^2((r^2+a^2)^2-a^2\Delta_r)-2aEL(r^2+a^2-\Delta_r)-L^2(\Delta_r-a^2)+\epsilon r^2\Delta_r=0$$

Solving the above equation for E and L, we have

$$E = \frac{aL\left(r^2+a^2-\Delta_r\right)\pm r\sqrt{\Delta_r\left(L^2r^2-\epsilon\left((r^2+a^2)^2-a^2\Delta_r\right)\right)}}{(r^2+a^2)^2-a^2\Delta_r}$$

$$L = \frac{-aE\left(r^2+a^2-\Delta_r\right)\pm r\sqrt{\Delta_r\left(E^2r^2+\epsilon\left(\Delta_r-a^2\right)\right)}}{\Delta_r-a^2}.$$

The following identity has been used to find the above results

$$\left[(r^2+a^2)^2-a^2\Delta_r\right]\left[\Delta_r-a^2\right]=r^4\Delta_r-a^2\left(r^2+a^2-\Delta_r\right)^2$$

We consider E = 1 (with unit rest mass at infinity) and the positive sign of E which requires $L < 0$ for $E < 0$ and

$$a^2L^2\left(r^2+a^2-\Delta_r\right)^2 > r^2\Delta_r\left[L^2r^2-\epsilon\left((r^2+a^2)^2-a^2\Delta_r\right)\right].$$

Using the equation of E, we can write

$$\left[(r^2+a^2)^2-a^2\Delta_r\right]\left[L^2\left(\Delta_r-a^2\right)-\epsilon r^2\Delta_r\right]<0.$$

It is clear from the above inequality that $L < 0$ corresponds to $E < 0$ and

$$\left(\frac{\Delta_r-a^2}{r^2}\right)<\frac{\epsilon\Delta_r}{L^2}.$$

The Original Penrose process

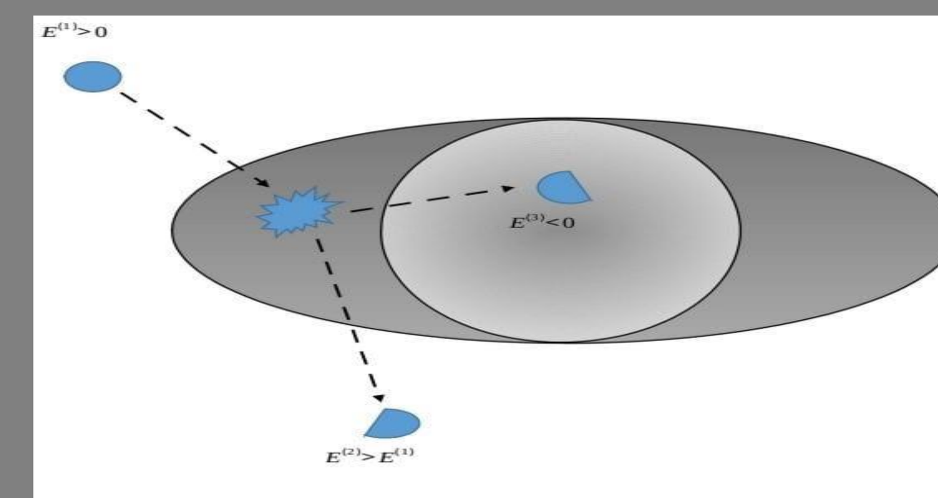

Figure 5 An illustration of Penrose process.

Let $E^{(x)}$ = 1, $L^{(x)}$; $E^{(y)}$, $L^{(y)}$ and $E^{(z)}$, $L^{(z)}$ be the energies and angular momenta. The angular momentum of the particle arrived from infinity by time-like geodesics can be obtained by setting E = 1 and ϵ = 1

$$L^x=\frac{-a(r^2+a^2-\Delta_r)\pm r\sqrt{\Delta_r(r^2-\Delta_r+a^2)}}{\Delta_r-a^2}=a^{(x)}$$

The relationship between energies and angular momenta can be obtained by choosing the negative and positive signs in the expression of L, as

$$L^{(y)}=\frac{-aE^{(y)}(r^2+a^2-\Delta_r)-E^{(y)}r^2\sqrt{\Delta_r}}{\Delta_r-a^2}=a^{(y)}E^{(y)},$$

$$L^{(z)}=\frac{-aE^{(z)}(r^2+a^2-\Delta_r)-E^{(z)}r^2\sqrt{\Delta_r}}{\Delta_r-a^2}=a^{(z)}E^{(z)}.$$

The conservation of energy and angular momentum yield

$$E^{(x)}=E^{(y)}+E^{(z)},$$
$$L^{(x)}=a^{(x)}=L^{(y)}+L^{(z)}=a^{(y)}E^{(y)}+a^{(z)}E^{(z)}.$$

Solving the above equations, we have

$$E^{(y)}=\frac{a^{(x)}-a^{(z)}}{a^{(y)}-a^{(z)}},\qquad E^{(z)}=\frac{a^{(y)}-a^{(x)}}{a^{(y)}-a^{(z)}}.$$

The Original Penrose Process

Inserting $a^{(x)}$, $a^{(y)}$ and $a^{(z)}$, we obtain

$$E^{(y)}=-\frac{1}{2}\left(\sqrt{\frac{(r^2+a^2)-\Delta_r}{r^2}}-1\right)$$

$$E^{(z)}=\frac{1}{2}\left(\sqrt{\frac{(r^2+a^2)-\Delta_r}{r^2}}-1\right).$$

The particle which escapes to infinity has more energy than the original particle $E^{(x)}$ = 1. Thus the gained energy (ΔE) can be written as

$$\Delta E=\frac{1}{2}\left(\sqrt{\frac{(r^2+a^2)-\Delta_r}{r^2}}-1\right)=-E^{(z)}.$$

At the event horizon, we have

$$\Delta E\leq\frac{1}{2}\left(\sqrt{1+\frac{a^2-\Delta_r}{r_+^2}}-1\right).$$

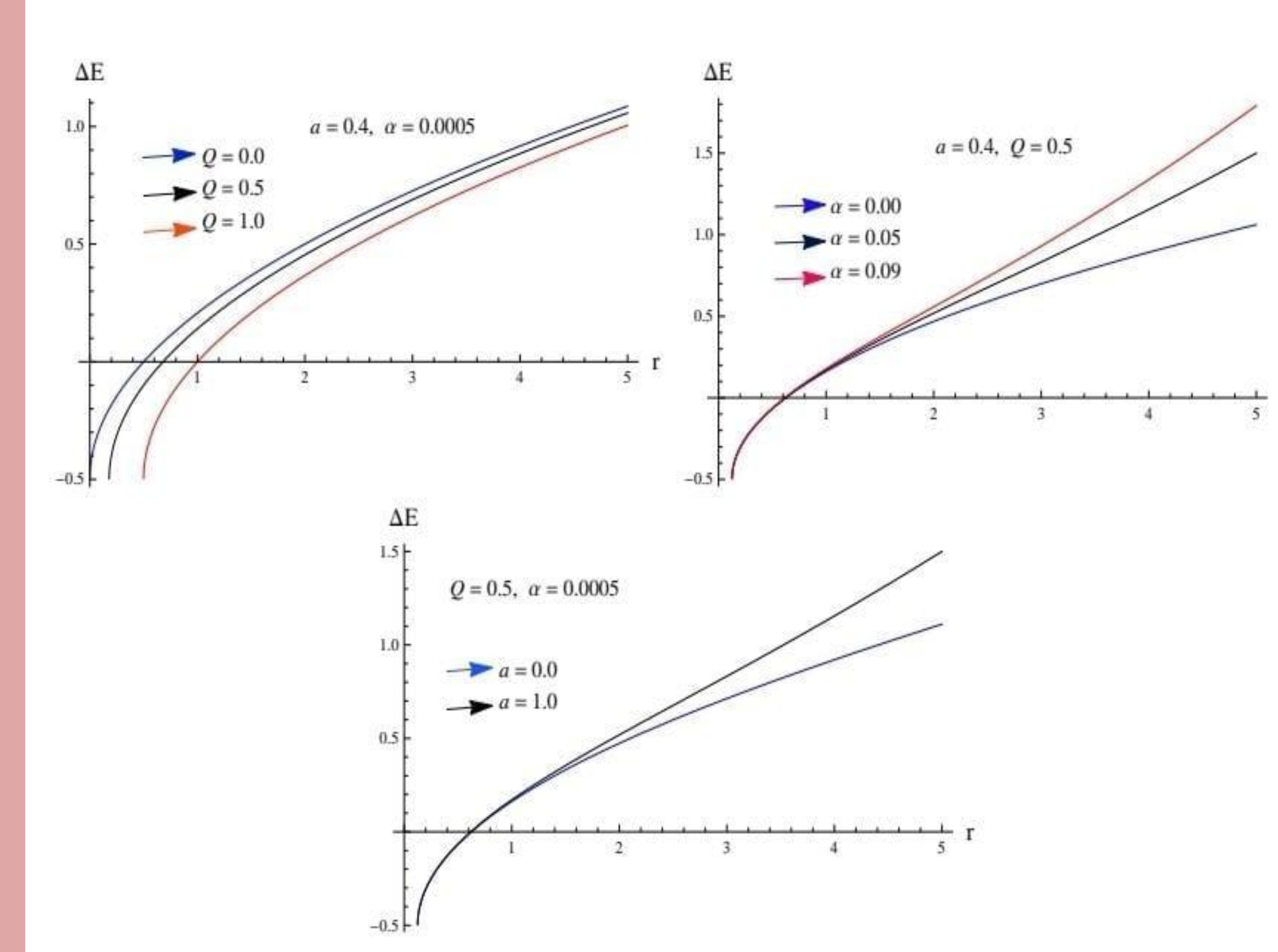

Figure 6 Plots of energy gain as a function of r.

Concluding Remarks

The graphs of energy have monotonic behavior and the descending and the rising curves correspond to the unstable and stable orbits similar to Kerr dS BH [Stuchl´ik, Z. and Slany´, P.: Phys. Rev. D **69**(2004) 064001].

We observe that particles for both direct and retrograde motion has less energy in the presence of dark energy as compared to its absence.

There is less angular momentum for direct orbit as compared to the retrograde orbits in the presence of dark energy which agrees with quintessential rotating BH [Toshmatov, B., Stuchl´ik, Z. and Ahmedov, B.: Eur. Phys. J. Plus **98**(2017)132].

We observe that the stable points never exceed the static radius in both null as well as time-like geodesics.

For the variation of a, the stable points always exceeds photon orbit (direct rotating) similar to the case of marginally stable orbits near Kerr dS BH [Stuchl´ik, Z., Charbula´k, D. and Schee, J.: Eur. Phys. J. C **78** (2018)180].

We found that more energy could be gained during the Penrose process in the presence of dark energy as well as with the increase rotation parameter